

Influence of Defects on the Angular Correlation of Positron-Annihilation Photons in Irradiated and in Deformed Iron[†]

C. L. Snead, Jr., and A. N. Goland

Brookhaven National Laboratory, Upton, New York 11973

and

J. H. Kusmiss, H. C. Huang, and R. Meade

Western Michigan University, Kalamazoo, Michigan 49001

(Received 19 August 1970)

Measurements of two-photon angular correlations following positron annihilation in both electron-irradiated and plastically deformed iron have been made at room temperature. The changes in the angular correlation observed for both treatments are similar and are attributed to the presence of vacancy-type defects. The changes due to the presence of these defects are analyzed in terms of the enhancement of the probability of annihilation of a positron with conduction electrons relative to annihilation with core electrons. The observed effects saturate with increasing defect concentration for both treatments, the total change being larger at saturation for the deformed specimen than for the irradiated one. This is interpreted as being due to less overlap of the positron wave function with core-electron wave functions at vacancy-agglomerate trapping sites in the deformed specimen than at the single-vacancy sites present in the irradiated sample. Stepwise annealing of the specimens firmly established a vacancy-positron interaction, which tends to localize positrons in the vicinity of vacancies, as responsible for the angular correlation changes observed. Arrival of carbon interstitial impurities at single-vacancy sites completely nullified the vacancy-positron interaction. The capture cross section of a vacancy for a positron in iron is estimated to be about $10 \times 10^{-16} \text{ cm}^2$. A method for deducing this cross section from a combination of lifetime and angular correlation results is presented in the Appendices. Recovery of the single vacancies present in the deformed specimen reduced the effect of the deformation by approximately one-half. Additional annealing to 400 °C reduced the effect further, but complete recovery was not achieved for the deformed sample up to this temperature.

I. INTRODUCTION

Several investigators have shown that changes occur in the two- γ angular correlation of electron-positron annihilation radiation following plastic deformation.¹⁻⁴ Since similar changes have been seen in metals at elevated temperatures using both angular correlation and lifetime measuring techniques,⁵⁻⁷ the vacancy was proposed^{3,8,9} as possibly being the cause of the observed effects. The interpretation put forward was that vacancies are attractive sites in the lattice for positrons, so that the likelihood of annihilation in the vicinities of these vacancies is increased. The absence of the core electrons in these regions weights the annihilation probabilities of positrons in favor of the conduction electrons. Strong evidence for this suspected role of vacancies accrued with the demonstration of similar effects produced by electron irradiation in platinum.¹⁰ Thus, the same argument may be applied to vacancy effects in metals whether the vacancies are generated thermally, by irradiation or by deformation.

Irradiations such as those described in Ref. 10, and also reported here, produce vacancy-interstitial pairs at the irradiation temperature of 95 °K. The

interstitial is mobile at this temperature and migrates freely until it is trapped at some site such as an impurity, or until it annihilates at a surface or with a vacancy. When the irradiated sample is warmed to room temperature, interstitials in shallow traps will anneal out, leaving only interstitials in deep traps and homogeneously distributed single vacancies, which are immobile until the sample temperature is elevated well above room temperature. The influence of the trapped interstitials on the angular correlation curve is not known, but evidence involving other atomic impurities in the lattice leads one to discount the contribution of interstitials to the changes observed. McKee, Langstroth, and MacKenzie,¹¹ in trying to explain the narrowing of the angular correlation curves for indium, zinc, and cadmium with elevated temperature, showed that the alloying of magnesium with indium and indium with lead for solute concentrations up to 28 at. % had relatively little effect on the angular correlation, and not nearly enough effect to account for the changes seen at the elevated temperatures. These changes can be attributed to the presence of lattice vacancies which are generated thermally in appreciable concentrations in these metals at fairly low temperatures, owing to

the relatively low energy of formation for vacancies. Interstitial hydrogen in titanium has been shown¹² to broaden slightly the angular correlation curve, which is just opposite to the result achieved by the addition of vacancies to the lattice. Contributions due to trapped self-interstitials, then, are not considered to have a significant effect upon the results presented here.

One should be able to ascertain the degree of responsibility of the vacancy for the effects seen in the irradiated metals by employing a series of thermal anneals, each followed by room-temperature angular correlation measurements. As the temperature at which vacancies become mobile and anneal out is approached and passed, any contribution to angular correlation effects by the vacancies should diminish. After an annealing treatment at temperatures above that for thermal activation of single-vacancy migration, all effects due to non-equilibrium concentrations of vacancies should have disappeared (assuming no trapping of migrating vacancies). This same tempering procedure is applicable to cold-worked metals with respect to non-equilibrium concentrations of vacancies produced by nonconservative jog motion through the lattice.

II. EXPERIMENTAL

Stepwise annealing procedures have been applied to both cold-worked and electron-irradiated iron specimens of 99.95% purity. Vacancy motion is believed to occur near 200 °C in iron¹³; hence, room-temperature angular correlation measurements to study the effects due to vacancies were possible. The iron specimens were all cut from the same sheet obtained from the Johnson-Matthey Co. to a size of $1 \times \frac{1}{4} \times 0.020$ in., and subsequently were annealed at 1150 °C in helium for 2 h. The cold working was accomplished by rolling the specimens at room temperature to the percentages of thickness reduction stated. Irradiation was performed with 2.5-MeV electrons from the Brookhaven Dynamitron accelerator with the samples immersed in liquid argon. The energy degradation of the beam traversing the sample was small compared to the beam energy, thereby assuring uniform defect production, whereas the lower-energy positrons were all stopped in the specimen. Windows made of $1.5 \times 1.5 \times 0.0006$ in. Havar¹⁴ were used for beam entrance and exit. Sample temperature during irradiation was monitored with a copper-constantan thermocouple spotwelded to the sample. Typically, 1 °K rises in temperature were seen for beam-current densities of 20–40 $\mu\text{A}/\text{cm}^2$. Total beam-current density was limited by the formation of a "vapor lock" around the specimen, causing the heat transfer to the bath to decrease drastically. When this phenomenon occurred, the sample temperature cycled between ~ -180 °C and several

hundred degrees centigrade at typically ~ 1 Hz. This behavior necessitated sample replacement.

The angular correlation apparatus used in these experiments at Western Michigan University included two 6-in.-long cylindrical NaI(Tl) detectors of 2.5-in. diam, which were placed 100 in. apart behind horizontal collimating slits. The source of positrons was 2.5 mCi of sodium-22 mounted above the sample but shielded from direct view of either detector by 7 in. of lead. The 0.020-in.-thick samples were tipped approximately 10° with respect to the horizontal in order to minimize the variation of γ -ray absorption in the sample over the angular correlation range. The over-all angular resolution of the apparatus was 1.1 mrad and the resolving time of the coincidence electronics was 30 nsec. All curves shown are normalized to the same total area and folded about the 180° position. The diameter of the circular data points or the height of the experimental points typically denotes two standard deviations from the mean counting rate at the peak of the distribution, with a random coincidence counting rate always less than 0.5% of the peak counting rate.

III. RESULTS AND DISCUSSION

A. Electron Irradiation

In Fig. 1 we show a comparison of the angular correlation for electron-irradiated iron for a dose of $1.0 \times 10^{19} \text{ e}^-/\text{cm}^2$ with that for an annealed undamaged specimen. For the curve depicting the results for the irradiated specimen, enhancement of the counting rate at small angles (low electron momenta), with the accompanying suppression at large angles, typifies the effects attributed to vacancy-type defects. The explanation of the origin of this effect as outlined in the Introduction is at present phenomenological. A vacancy is created by the removal of a positively charged ion from a lattice site. The region of the vacancy, now negative with respect to the unperturbed lattice, experiences an attractive Coulomb interaction with the positron, thereby causing the positron to spend more time in the vicinity of the vacancy, and thereby increasing the probability of annihilation in this region rather than elsewhere in the lattice. The extent to which a positron is actually trapped at a vacancy has recently been investigated by Hodges.¹⁵ The enhanced annihilation probability at vacancy sites has two measurable manifestations. First, annihilations at these sites will more likely involve conduction electrons than core electrons due to the absence of the ions. This shows up (see Fig. 1) as an increase in the number of annihilation events at small angles. Normalization of the curves to the same total area produces a compensating decrease in the counting rate at large angles. The number of annihilation events shifted from large

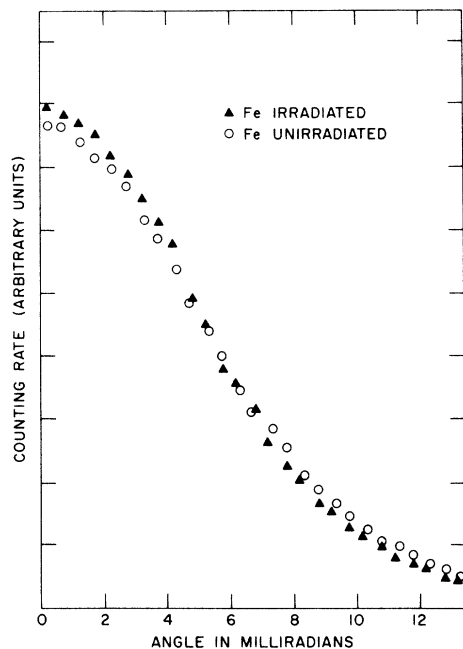


FIG. 1. Comparison of angular correlation curves for irradiated and unirradiated iron measured at room temperature. Irradiation dose was $1.0 \times 10^{19} \text{ e}^-/\text{cm}^2$ at 90°K followed by an anneal to room temperature.

to small angles should increase with increasing vacancy concentration (for low concentrations).

Second, the presence of vacancies in a metal should also affect the lifetime of positrons.^{7,8} A positron annihilating at a vacancy site samples an electron density which is lower than the average for the metal because of the absence of the core electrons associated with the missing ion, and also because the vacancy is a region of higher potential energy for the conduction electrons.

If the effects seen in Fig. 1 are indeed due to irradiation-induced vacancies, thermal anneals to temperatures above the point at which vacancies are mobile should anneal out the vacancies and restore the angular correlation curve to its original preirradiation shape. The temperature for vacancy migration in iron is believed to be $\sim 200^\circ\text{C}$, with $E_m = 1.1 \text{ eV}$.¹³

Figure 2 shows the effect on the angular correlation of a 1-h anneal of the irradiated specimen at 100°C in air. The changes induced by the irradiation have been completely removed by this treatment, even though the annealing temperature was below that for which vacancies should be mobile. Recovery of irradiation damage over this temperature range has, however, been observed previously and explained as due to carbon interstitial impurities diffusing to and being trapped by vacancies at $\sim 50^\circ\text{C}$.¹⁶ From our results it seems likely that

the arrival of a carbon atom at a vacancy site nullified the charge imbalance that gives rise to the positron-vacancy attractive interaction, thereby causing the disappearance of the vacancy-caused effect. That complete recovery was realized implies that the concentration of diffusing carbon impurities was comparable with, or greater than, the vacancy concentration introduced. Defect-production data for electron-irradiated iron are scarce; the best estimate of the defect concentration in the samples used in the present work is made by comparison with a similar radiation treatment reported by Neely and Keefer.¹⁷ They irradiated iron to a "high dose" with 1.3-MeV electrons at 4.2°K and then annealed it to 185°K . No flux data were given. The residual resistivity following this treatment was $1.3 \times 10^{-8} \Omega\text{cm}$; using a value of $12.5 \mu\Omega\text{cm/at.}\%$ for Frenkel pairs,¹⁸ one estimates a concentration of 10 ppm. Since many of the migrating interstitials have annihilated at surfaces or other sinks, or have been trapped at impurities and therefore probably contribute to a lesser extent to the defect resistivity, most of the resistivity contribution at 185°K will be due to the vacancies still remaining. This indicates a vacancy concentration perhaps a factor of 2 higher than 10 ppm. For our irradiations of less pure iron with higher-energy electrons and for a dose ($1.0 \times 10^{19} \text{ e}^-/\text{cm}^2$) perhaps higher than the one above, an estimate of 10–20 ppm is not unreasonable for the vacancy concentration at room temperature. For the iron specimens used in this work a carbon content of

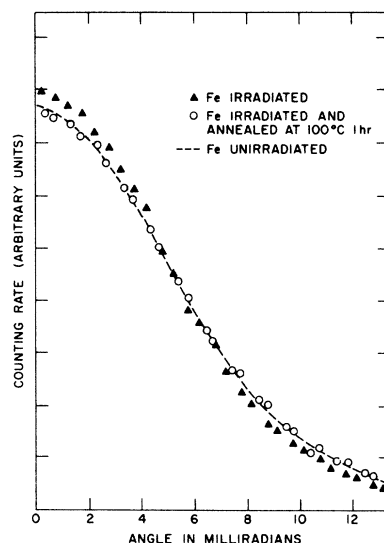


FIG. 2. Angular correlation curves comparing irradiated iron with iron irradiated and then annealed at 100°C for 1 h. The dashed curve depicts the angular correlation for the annealed unirradiated specimen.

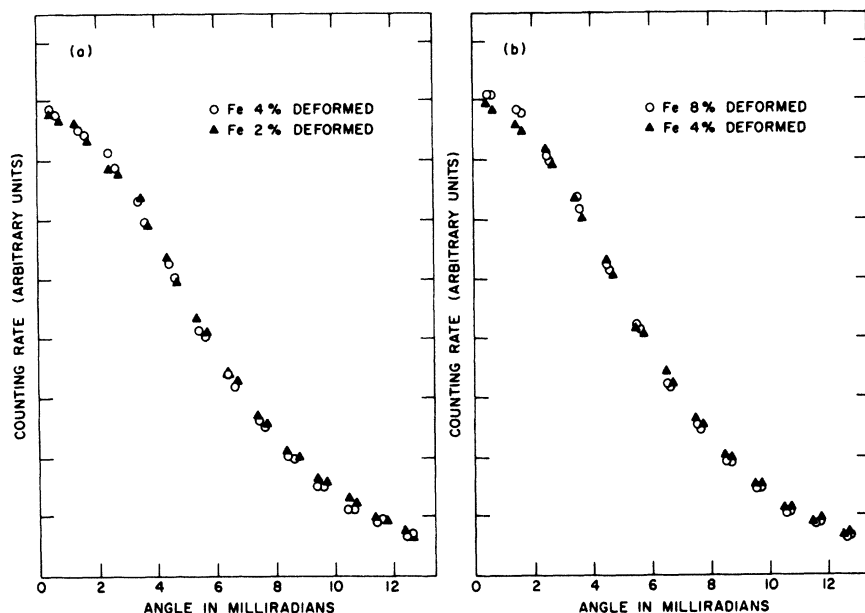


FIG. 3. Comparison of angular correlation curves for progressively higher deformations: (a) shows 2% versus 4% and (b) shows 4% versus 8%. Percentages are for thickness reduction.

50 ± 5 ppm was determined subsequently by neutron-activation analysis. This concentration is sufficiently large so that every vacancy can trap a carbon atom. Computer studies suggest that the position of the trapped carbon atom is close to the center of the vacancy, rather than in an interstitial position.¹⁹

B. Plastic Deformation

Similar procedures can be applied toward understanding the mechanisms responsible for the changes seen in angular correlation measurements of deformed metals. Figure 3 shows the progressively larger changes seen for successively higher percentages of deformation in iron. Cuddy^{20,21} has shown that except for an initial high rate of increase for deformations up to 5%, the resistivity attributed to point defects created by deformation of iron increases linearly with the deformation. The rate of increase of the effect shown in Fig. 3 is approximately linear up to deformations of 8%. As shown by Fig. 4, further deformation to 16% produces relatively little increase in the height of the curve, certainly not double the change already induced as would be suggested by a continued linear rise, indicating a tendency toward saturation of the effect between 8 and 16% deformation. The total deformation-induced effect is shown in Fig. 5. Saturation effects have been seen also in deformed platinum¹⁰ and nickel²² at about the same deformation levels. Indeed, the angular correlation curve for nickel grossly deformed to 45% was nearly identical to a 16% curve.

Lattice damage created by cold-rolling iron at room temperature appears chiefly as tangles of dis-

locations associated with vacancy dislocation loops clustered nearby,²³ and vacancy complexes ranging from single to multiple ones which are generated by nonconservative motion of jogs through the lattice.²⁴ The best evidence to date for the migration temperature of vacancies (single vacancies and divacancies are thought to move with approximately

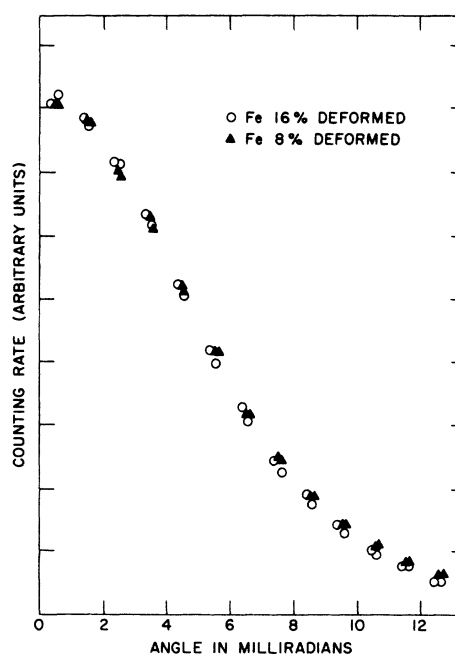


FIG. 4. Comparison of angular correlation curves for 8% and 16% plastically deformed iron.

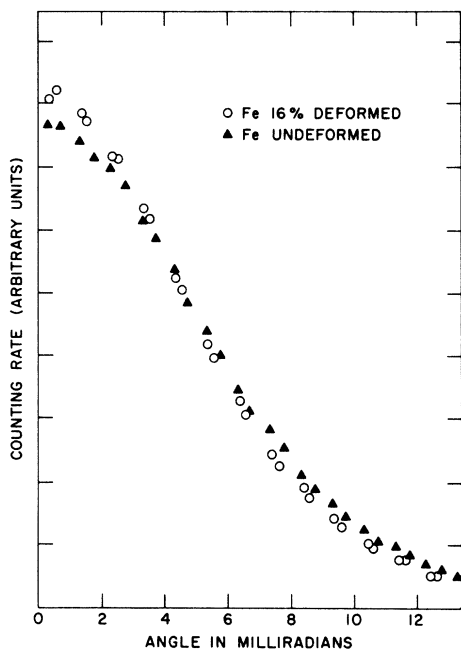


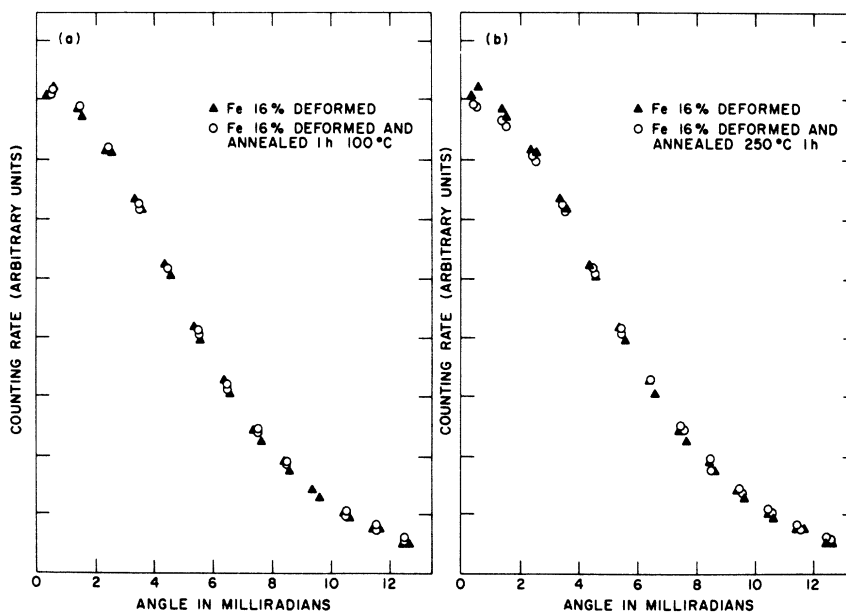
FIG. 5. Comparison of angular correlation curve for iron plastically deformed to 16% with an undeformed annealed specimen.

the same motion energy in bcc materials)²⁵ in iron comes from the quenching and cold-working results of Glaeser and Wever.¹³ They find stage III recovery in the range $27^{\circ}\text{C} < T < 127^{\circ}\text{C}$, which they attribute to carbon impurities migrating to vacancies and subsequent migration of the carbon-vacancy

complex, and a stage IV recovery in the range $127^{\circ}\text{C} < T < 247^{\circ}\text{C}$ corresponding to the migration of single vacancies. Therefore, an anneal to 250°C should remove all the single vacancies and divacancies, barring trapping, and the angular correlation effects associated with these defects should disappear as a consequence. Anneals may be conducted to 400°C with only slight alteration of the dislocation networks present. Since recrystallization in iron begins at 450°C or higher, such anneals affect only free or loosely trapped vacancies and their related effects, leaving effects that are attributable to the dislocations intact.

The annealing results for cold-worked iron are shown in Figs. 6 and 7. The 100°C anneal shown in Fig. 6(a) causes essentially no change in the curve for the 16% deformed specimen. From the change in resistivity remaining at room temperature following liquid-nitrogen-temperature deformations of iron samples most similar in purity to those used here, a value between 2.5 and $5.0 \times 10^{-8} \Omega \text{ cm}$ for 16% deformation is reported by Cuddy.²⁰ This yields values of 20–40 ppm of vacancies. These values are certainly lower than the total vacancy concentration in the lattice because vacancies present in dislocation loops and clusters contribute less to the resistivity than an equivalent number of isolated single vacancies. However, they do give an upper limit to the concentration of single vacancies distributed throughout the lattice. The migration of interstitial carbon impurities to vacancy sites is complicated by the presence of clusters and dislocations at which the carbon atoms also might become trapped. In fact, a large number of the carbon impurities could become associated with the

FIG. 6. The effects of annealing the deformed iron are depicted in (a), where the angular correlation for the specimen deformed 16% is compared with the angular correlation for the specimen deformed 16% and then annealed at 100°C for 1 h. (b) compares the angular correlation for the specimen deformed 16% with the angular correlation for the specimen deformed 16% and annealed at 250°C for 1 h.



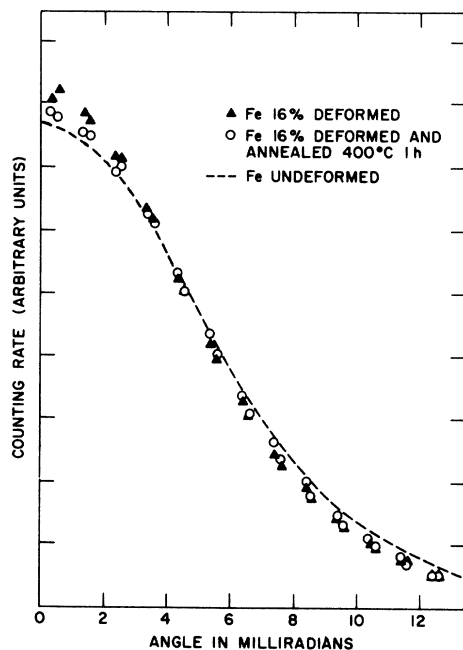


FIG. 7. Comparison of angular correlation curves for 16% deformed iron with that for the 16% deformed specimen annealed at 400 °C for 1 h. The dashed curve is the angular correlation for the undeformed iron sample.

dislocations during the motion of the latter during the cold working. Thus, the negligible recovery due to carbon migration relative to that observed in the irradiated sample might be explained by the existence of these competing processes. Also, since saturation has been essentially realized in the 16% deformed sample, removal of the vacancies in excess of the saturation level is necessary before any decrease of the peak enhancement could be seen. Both of the above mechanisms are probably responsible for the absence of recovery comparable to that of the irradiated specimen for an anneal of 100 °C.

The results of annealing above 100 °C are shown in Figs. 6(b) and 7 for 1-h anneals at 250° and 400 °C, respectively. The majority of the recovery takes place during the 250 °C anneal, a temperature at which single vacancies and divacancies are mobile. A small amount of additional recovery takes place following the 400 °C anneal. This is consistent with the continuing resistivity recovery seen in cold-worked iron by Cuddy^{20,21,26} in the same temperature range. Vacancy removal comes about in this temperature range probably through the breakup of small vacancy clusters or the agglomeration of small clusters into larger ones as seen in electron microscope studies of neutron-irradiated bcc metals.²⁷ Thus the continuing annealing treatment removes the vacancy-type effects which act as

attractive sites for positrons, starting with single-vacancy neutralization by carbon atoms at 100 °C. This is followed by single-vacancy migration at 250 °C and reduction of small clusters at temperatures up to 400 °C. Above 400 °C only large clusters²⁷⁻³⁰ of dislocation loops and dislocation tangles²³ with which the positrons can interact remain. The amount of angular correlation change due to these remaining defects is shown in Fig. 7, in which the results for the sample deformed 16% and annealed to 400 °C are compared to the results for the annealed undamaged specimen.

It should be pointed out here that there could be another phenomenon taking place during the anneals which would influence the recovery of the induced effects similarly to a decrease in the concentration of trapping sites for positrons. We postulate that a decrease in the size of a vacancy cluster should cause a decrease in the capture cross section for thermalized positrons and should also further decrease the probability that a positron annihilating in the neighborhood of the cluster annihilates with a conduction electron. The enhancement beyond that due to a single vacancy is strictly a size effect in which the wave function of a positron in a large vacancy void overlaps neighboring core-electron wave functions to a lesser extent than it does when the positron is localized at a single vacancy. Thus, when a void decreases in size, there is an increase in the probability of annihilation with core electrons for a positron in the void.

To the extent that it is valid to consider the angular correlation curve as the sum of two components, one a nearly parabolic distribution due to positron annihilations with conduction electrons, and the other an approximately Gaussian-shaped distribution due to core-electron annihilations, one can, in principle, define a relative probability, P , equal to the ratio of the areas under the two contributing curves: viz., P equals the area under the narrow distribution divided by the area under the broad distribution. Determination of the respective areas under these curves is, however, quite difficult. When the total area under each angular correlation curve is normalized to the same value, changes in P are reflected in changes in the maximum counting rate. The change of the maximum counting rate can be shown to be directly proportional to the change in the area under the narrow distribution (assumed to be parabolic). Thus, the larger the ordinate at 0 mrad, the larger the value assigned to P . As shown in Appendix A, the change in the peak height of the angular correlation curve can be used to calculate the capture cross section of a vacancy for a positron and yields a value of approximately $10 \times 10^{-16} \text{ cm}^2$.

Let a be the area under the narrow component and b be the area under the wide component. We define the ratio of these two components as

$$a/b = P. \quad (1)$$

For a perfect metallic crystal, the probability that an annihilation will contribute to the a component is the same throughout the crystal, and we call this probability p_L . The two components are $a_L = Cp_L$ and $b_L = C(1 - p_L)$, where C is the total number of annihilations contributing to the entire angular correlation curve measured. Thus, for the case of a perfect lattice, we have

$$a_L/b_L = p_L/(1 - p_L) \equiv P_L. \quad (2)$$

For the case of the irradiated specimen, the area under the angular correlation curve is made up of four components, narrow components from annihilations in the unperturbed lattice and also at sites of single vacancies distributed homogeneously throughout the lattice, and wide components from these two annihilation regions. The ratio of narrow to wide component areas for this case is

$$\frac{a}{b} \Big|_{\text{irrad}} = \frac{a_L + a_{1v}}{b_L + b_{1v}}, \quad (3)$$

where a_{1v} is the area component due to annihilation with conduction electrons at a single vacancy and b_{1v} is the component due to core-state annihilations at a single vacancy. Let p_{1v} be the probability that an annihilation at a single vacancy contributes to the a_{1v} component, and let C_T be the fraction of positron annihilations occurring at defect trapping sites (single vacancies in this special case). Then we have

$$\frac{a}{b} \Big|_{\text{irrad}} = \frac{(1 - C_T)p_L + C_T p_{1v}}{(1 - C_T)(1 - p_L) + C_T(1 - p_{1v})}. \quad (4)$$

As the relative number of annihilations at vacancies C_T increases from zero, changes in a/b from the perfect lattice value will be determined by the ratio of p_L to p_{1v} . For $p_L < p_{1v}$, increases in a/b as measured by the zero mrad intercept of the angular correlation curve are predicted with increasing vacancy concentration. For $p_L > p_{1v}$, a decrease of a/b is predicted. For the case of irradiated iron, a/b increased with C_T (Fig. 1) confirming $p_{1v} > p_L$, i.e., a higher probability of annihilations with conduction electrons at a vacancy site than in the unperturbed lattice.

Comparison of the vacancy concentration determined for the irradiated specimen with that of the most deformed specimen leads to the conclusion that the vacancy concentration in the irradiated sample is near saturation. When the effect saturates, corresponding to $C_T \rightarrow 1$, we have

$$\frac{a}{b} \Big|_{\text{irrad}} = \frac{p_{1v}}{1 - p_{1v}} = P_T. \quad (5)$$

For the case of deformed iron, the possibility that p is a function of the size of the vacancy-type defect at which the positron annihilates, as discussed above, must be considered. The ratio of the areas of the narrow and wide distributions in this case will be

$$\frac{a}{b} \Big|_{\text{def}} = \left(a_L + \sum_{i=1}^N a_i \right) / \left(b_L + \sum_{i=1}^N b_i \right) \quad (6)$$

where the area under the angular correlation curve is the sum of all the components,

$$a + b = a_L + b_L + \sum_{i=1}^N a_i + \sum_{i=1}^N b_i. \quad (7)$$

The a_i and b_i are the conduction and core components, respectively, of the i th type of complex. It is assumed that there are N types of complexes with differing a_i to b_i ratios. If p_i is the probability that an annihilation in the i th type of complex contributes to a_i , then Eq. (6) becomes

$$\frac{a}{b} \Big|_{\text{def}} = \frac{\left[(1 - C_T)p_L + \sum_{i=1}^N C_i p_i \right]}{\left[(1 - C_T)(1 - p_L) + \sum_{i=1}^N C_i(1 - p_i) \right]}, \quad (8)$$

where C_i is the fraction of the annihilations taking place at the i th complex and $\sum_{i=1}^N C_i = C_T$. Since the damage created by deformation is inhomogeneous and the distribution of the i th types of complexes is an unknown quantity, we will use an averaging process in which we let

$$\sum_{i=1}^N C_i \bar{p}_i = C_T \bar{p}_d \quad \text{and} \quad \sum_{i=1}^N C_i(1 - \bar{p}_i) = C_T(1 - \bar{p}_d), \quad (9)$$

where \bar{p}_d is an average probability that an annihilation at a complex will contribute to the conduction area. When substituted into Eq. (8) the quantities defined above give

$$\frac{a}{b} \Big|_{\text{def}} = \frac{(1 - C_T)p_L + C_T \bar{p}_d}{(1 - C_T)(1 - \bar{p}_d) + C_T(1 - \bar{p}_d)}. \quad (10)$$

Equation (10) is seen to be of the same form as Eq. (4) describing the ratio for the irradiated specimen, but with the average \bar{p}_d in place of p_{1v} . The relative values of these last two numbers can be gauged by comparing the maximum counting rates for the irradiated (Fig. 1) and deformed (Fig. 5) specimens at defect concentrations which produce a saturation of the effects seen. At saturation, we have $C_T \rightarrow 1$, which yields

$$\frac{a}{b} \Big|_{\text{def}} \rightarrow \frac{\bar{p}_d}{1 - \bar{p}_d} = \bar{P}_T. \quad (11)$$

The implication of the higher value of intercept for the deformed specimen is that

$$\bar{P}_T > P_T,$$

which is a restatement of the contention that on the

average core-electron wave functions of neighboring lattice atoms extend into the volume of a single vacancy to a greater extent than they do into vacancy-agglomerate volumes of larger size.

The significance of $\bar{P}_T > P_T$ in the interpretation of the annealing results in the deformed specimen is that either a reduction in the average size of the trapping sites or a reduction in the concentration of trapping sites would have similar manifestations in the angular correlation after annealing. Both processes are probably occurring during the 250 and 400 °C anneals.

IV. SUMMARY

The irradiation-induced effects are completely recovered after an anneal to 100 °C owing to the arrival of carbon atoms at vacancies during this anneal. The complete removal of the vacancy effects on angular correlation is attributed to the occupation by carbon atoms of essentially all of the vacancies created by the irradiation.

The 100 °C anneal in the deformed specimen with the ensuing migration of carbon interstitial impurities produces none of the recovery observed in the irradiated sample. We suspect that this is due to the multiplicity of diverse trapping sites available to the carbon atoms in the heavily deformed lattice. Trapping of a carbon atom at a dislocation or at a large defect cluster should produce no appreciable change in the positron-defect attractive interaction. Just how effective a carbon ion might be in "neutralizing" a small vacancy complex is at this point speculative. Owing to the high concentration of extended defects in the deformed specimen, relatively few carbon atoms find single vacancies.

Annealing to 250 °C enabled single vacancies and divacancies to disappear from the lattice. The size of the recovery due to this removal and reduction of the concentration of trapping sites is mitigated somewhat by the arrival of some of these defects at larger nucleation centers for agglomerates, thereby raising the p_i for some of these complexes and consequently \bar{P}_T also. The relative importance of these two competing processes might be ascertained by conducting high-resolution electron microscopy in conjunction with the kinds of measurements reported here. From the amount of recovery observed due to the 250 °C anneal, however, it appears that there is a large decrease in concentration of defects which overshadows the growth phenomenon.

The anneal to 400 °C results in dissolution of smaller clusters and growth of larger ones as well as growth of the loops (Frank sessile) that are present. After the 400 °C anneal, the change in the angular correlation which remains unrecovered is due to loops, dislocation tangles, and voids.

Here again, further information regarding positron interactions with defects might be obtained by employing concurrent electron microscopy.

V. CONCLUSIONS

(a) Changes seen in the angular correlation curve due to both electron irradiation and deformation are attributed to positron-electron annihilations in the vicinity of vacancy-type defects.

(b) The effect of irradiation or deformation on the angular correlation is an increase in the probability of annihilations of positrons with conduction electrons in the vicinity of the defect.

(c) It seems reasonable to conclude that the conduction electron-positron annihilation rate increases with increasing average size of a vacancy agglomerate or dislocation loop.

(d) Saturation of the increase in height of the angular correlation curve occurs for single-vacancy concentrations on the order of 20 ppm.

(e) The arrival of a carbon atom at a single vacancy reduces the positron-vacancy interaction essentially to zero. To account for this complete deactivation, it appears that the carbon atom should be considered a substitutional impurity in the final trapped configuration rather than an interstitial impurity trapped at a lattice vacancy. That the vacancy is the point defect which pins the migrating carbon at ~50 °C is confirmed.

(f) A great many of the vacancy-type defects created by cold work in alpha iron at room temperature are single vacancies and divacancies (~40%) as seen by the amount of recovery due to the 250 °C anneal.

(g) An order-of-magnitude calculation of the capture cross section of a vacancy for thermalized positrons gives a value of $10 \times 10^{-16} \text{ cm}^2$.

(h) Positron annihilation techniques have been shown to offer a useful approach to investigations of vacancy-type defects. Separation of vacancy effects from those due to other lattice defects should prove quite useful in many defect studies.

APPENDIX A

In this appendix we outline a method of calculating the cross section for capture of a positron by a vacancy. It can be shown (see Appendix B) that the change in the peak height of the angular correlation curve with vacancy concentration can be written as

$$\Delta H = (\Delta H)_s \eta_t, \quad (\text{A1})$$

where $(\Delta H)_s$ is the difference in the peak heights for saturation and zero vacancy concentrations, and η_t is the fraction of annihilation events resulting from positrons which are trapped at vacancies. The fraction of annihilations due to trapped positrons can be calculated according to the model first pro-

posed by Brandt.³¹ The number of positrons η_1 which are trapped at time t is given by

$$n_1(t) = \frac{\lambda_1 \mu c N}{\lambda_2 - \lambda_1 + \mu c} [e^{-\lambda_1 t} - e^{-(\lambda_2 + \mu c) t}] \quad (A2)$$

where λ_1 and λ_2 are the decay constants for trapped and free positrons, respectively, μc is the trapping rate (assumed to be directly proportional to the concentration of vacancies c), and N is the total number of positrons.

In order to obtain the total number of annihilations from traps, it is necessary to integrate the instantaneous rate of annihilations from traps $\lambda_1 n_1(t)$ with respect to time. Since the time taken for an angular correlation experiment is essentially infinite, the result for the fraction of the total number of annihilations which come from positrons in traps is

$$\eta_t = \frac{1}{N} \int_0^\infty \lambda_1 n_1(t) dt = \frac{\mu c}{\lambda_2 + \mu c} \quad (A3)$$

The constant of proportionality between the trapping rate and the vacancy concentration can be written as

$$\mu = \sigma \bar{v} \quad (A4)$$

where σ is the cross section for trapping of a positron by a vacancy and \bar{v} is the speed of a thermalized positron. We take \bar{v} to be

$$\bar{v} = (2kT/m)^{1/2} = 9.5 \times 10^6 \text{ cm/sec.} \quad (A5)$$

From equations (A1), (A3), and (A4) it follows that

$$\begin{aligned} \sigma &= \lambda_2 \eta_t / \bar{v} c (1 - \eta_t) \\ &= \lambda_2 [\Delta H / (\Delta H)_s] / \bar{v} c [1 - \Delta H / (\Delta H)_s] \quad (A6) \end{aligned}$$

To be able to calculate σ one must measure the angular correlation for a series of specimens with a range of known vacancy concentrations from zero to the saturation value. In the case of plastic deformation experiments this is not possible; first, because the angular correlation changes have a mixture of contributions from extended defects as well as single vacancies, and second, because the dependence of the concentration of single vacancies on the plastic strain is not known for iron. However, from the data available we have calculated σ in two different ways.

In the first case we use the value of ΔH obtained for our irradiated specimen and $(\Delta H)_s$ from the deformation experiments [on the assumption that $(\Delta H)_s$ does not depend greatly on the mixture of defect types which are present]. The vacancy concentration is estimated from the work of Neely and Keefer¹⁷ to be $8.5\text{--}17 \times 10^{17} \text{ cm}^{-3}$. For λ_2 we use $6.25 \times 10^9 \text{ sec}^{-1}$ from the work of Weisberg.³² The resulting cross section is $\approx 2\text{--}6 \times 10^{-16} \text{ cm}^2$.

In the second case we use a value of $\Delta H / (\Delta H)_s$

derived from the angular correlation curves for the 16% deformed specimen and for the 16% deformed specimen after annealing at 250 °C. Presumably the change in peak height upon annealing is attributable to vacancies alone. From data presented by Cuddy²⁰ we estimate a vacancy concentration of $1.8 \times 10^{18} \text{ cm}^{-3}$ for 16% plastic deformation. The resulting cross section is $\approx 2.5 \times 10^{-16} \text{ cm}^2$.

The order-of-magnitude agreement between the cross sections calculated according to the two different methods given above is encouraging in view of the various uncertainties involved. In the first case, the use of $(\Delta H)_s$ from the deformation data leads to an underestimate of σ , since we would expect $(\Delta H)_s$ to be smaller when only single vacancies are present in the specimen. Taking $(\Delta H)_s$ for vacancies alone to be 50% smaller than the deformation value would make σ three times larger. In the second case, we have used a vacancy concentration for the deformed specimen which is probably too small because during the annealing process some vacancies migrate to dislocations and still contribute to the resistivity to some extent. Thus, the effect of assuming that the change of resistivity upon annealing quoted by Cuddy represents the change in the vacancy concentration is to yield an overestimate of the trapping cross section. In view of these uncertainties, we conclude that a reasonable estimate of the capture cross section is approximately $10 \times 10^{-16} \text{ cm}^2$. It is somewhat surprising that this value of the trapping cross section for Fe is considerably smaller than the value of $340 \times 10^{-16} \text{ cm}^2$ for Al derived by Hautojärvi *et al.*³³ from lifetime data. Obviously considerably more experimental and theoretical work must be done to clarify the nature of the interactions between defects and positrons in metals.

APPENDIX B

Let the angular correlation curve $H(\theta)$ be represented by the sum of a parabola $A(\theta)$ and a Gaussian $B(\theta)$:

$$H(\theta) = A(\theta) + B(\theta) = h_a [1 - (\theta^2 / \theta_F^2)] + h_b e^{-k^2 \theta^2} \quad (B1)$$

where θ_F is the Fermi cutoff angle, h_a and h_b are the values of $A(0)$ and $B(0)$, respectively, and k is a constant which characterizes the width of the Gaussian. If a and b are the areas under the parabola and Gaussian, respectively, it can easily be shown that

$$h_a = \alpha a, \quad h_b = \beta b \quad (B2)$$

where $\alpha = 3/(4\theta_F)$ and $\beta = k/\sqrt{\pi}$. Let H' and H be the peak counting rates for two different defect concentrations. If α and β do not change with defect concentration, and if $\alpha + \beta$ is held constant, it follows that

$$\Delta H = H' - H = (\alpha - \beta)(a' - a) \quad (B3)$$

The area σ' under the narrow part of the angular correlation curve for the higher defect concentration can be written as

$$a' = \eta_f f_a N + \eta_t f_a' N = (1 - \eta_t) f_a N + \eta_t f_a' N, \quad (\text{B4})$$

where η_f = fraction of free positrons which annihilate, η_t = fraction of trapped positrons which annihilate, N = total number of annihilations, f_a = probability that an annihilation of a free positron will contribute to the narrow distribution, f_a' = probability that an annihilation of a trapped positron will contribute to the narrow distribution. The area a_0 under the narrow part of the angular distribution for a specimen with zero concentration of defects becomes simply

$$a_0 = f_a N. \quad (\text{B5})$$

From equations (B3), (B4), and (B5) it follows that

$$\Delta H = (\alpha - \beta) (a' - a_0) = (\alpha - \beta) \eta_t N (f_a' - f_a). \quad (\text{B6})$$

For a saturation concentration of defects,

$$\eta_t = 1, \quad (\Delta H)_s = (\alpha - \beta) N (f_a' - f_a), \quad (\text{B7})$$

and hence

$$\Delta H = (\Delta H)_s \eta_t,$$

where $(\Delta H)_s$ is a constant equal to the difference in the number of counts at the peak at saturation and at zero concentration of vacancies. A somewhat similar analysis has been employed recently by Triftshauser *et al.*³⁴ to derive the vacancy formation energy from measurements of the temperature dependence of the two-photon angular correlation.

[†]Work supported by the U. S. Atomic Energy Commission.

¹I. Ya. Dekhtyar, D. A. Levina, and V. S. Mikhalekov, Dokl. Akad. Nauk SSSR **156**, 795 (1967) [Soviet Phys. Doklady **9**, 492 (1964)].

²I. Ya. Dekhtyar, V. S. Mikhalekov, and S. G. Sakharova, Dokl. Akad. Nauk SSSR **168**, 785 (1966) [Soviet Phys. Doklady **11**, 537 (1966)].

³S. Berko and J. C. Erskine, Phys. Rev. Letters **19**, 307 (1967).

⁴A. A. Adamenko, I. Ya. Dekhtyar, and V. S. Mikhalekov, Phys. Letters **26A**, 288 (1968).

⁵A. T. Stewart, J. H. Kusmiss, and R. H. March, Phys. Rev. **132**, 495 (1963).

⁶I. K. MacKenzie, G. F. O. Langstroth, B. T. A. McKee, and O. G. White, Can. J. Phys. **42**, 1837 (1964).

⁷W. Brandt and H. F. Waung, Phys. Letters **27A**, 700 (1968).

⁸I. K. MacKenzie, T. L. Khoo, A. B. MacDonald, and B. T. A. McKee, Phys. Rev. Letters **19**, 946 (1967).

⁹I. K. MacKenzie, Phys. Letters **30A**, 115 (1969).

¹⁰J. H. Kusmiss, C. D. Esseltine, C. L. Snead, Jr., and A. N. Goland, Phys. Letters **32A**, 175 (1970).

¹¹B. T. A. McKee, G. F. O. Langstroth, and I. K. MacKenzie, in *Positron Annihilation*, edited by A. T. Stewart and L. O. Roellig (Academic, New York, 1967), p. 281.

¹²J. Wesolowski, B. Rozenfeld, and M. Szuszkiewicz, Acta Phys. Polon. **24**, 729 (1963).

¹³W. Glaeser and H. Wever, Kernforschungsanlage Jülich Report No. Jül-Conf-2, 1968, Vol. II (unpublished).

¹⁴Precision Metals Division, Hamilton Watch Co., Lancaster, Pennsylvania.

¹⁵C. H. Hodges, Phys. Rev. Letters **25**, 284 (1970).

¹⁶F. E. Fujita and A. Damask, Acta Met. **12**, 331 (1964).

¹⁷H. H. Neely and D. W. Keefer, Phys. Status Solidi **24**, 217 (1967).

¹⁸P. Lucasson and R. M. Walker, Phys. Rev. **127**, 485 (1962).

¹⁹R. A. Johnson, G. J. Dienes, and A. C. Damask, Acta Met. **12**, 1215 (1964).

²⁰L. J. Cuddy, Phil. Mag. **12**, 855 (1965).

²¹L. J. Cuddy, Acta Met. **16**, 23 (1968).

²²C. L. Snead, Jr., A. N. Goland, H. C. Huang, C. D. Esseltine, R. Meade, and J. H. Kusmiss, Bull. Am. Phys. Soc. **15**, 300 (1970).

²³S. M. Ohr and D. N. Beshers, Phil. Mag. **10**, 219 (1964).

²⁴P. B. Hirsch, Phil. Mag. **7**, 67 (1962).

²⁵R. A. Johnson, Phys. Rev. **134**, A1329 (1964).

²⁶L. J. Cuddy and J. C. Raley, Acta Met. **14**, 440 (1966).

²⁷B. L. Eyre and A. F. Bartlett, Phil. Mag. **12**, 261 (1965).

²⁸D. M. Maher and B. L. Eyre, Phil. Mag. **17**, 1 (1968).

²⁹J. D. Meakin and J. G. Greenfield, Phil. Mag. **11**, 277 (1965).

³⁰B. L. Eyre and M. E. Downey, Atomic Energy Research Establishment Report No. AERE-R 5269, 1966 (unpublished).

³¹W. Brandt, in *Positron Annihilation*, edited by A. T. Stewart and L. O. Roellig (Academic, New York, 1967), p. 180.

³²H. Weisberg, Ph. D. thesis, Brandeis University, 1965 (unpublished).

³³P. Hautojärvi, A. Tamminen, and P. Jauko, Phys. Rev. Letters **24**, 459 (1970).

³⁴W. Triftshauser, B. T. A. McKee, and A. T. Stewart, Bull. Am. Phys. Soc. **15**, 812 (1970).